

# A model of light collimation by photonic crystal surface modes

Wojciech Śmigaj\*

Surface Physics Division, Faculty of Physics,  
Adam Mickiewicz University,  
Umultowska 85, 61-614 Poznań, Poland

We propose a quantitative model explaining the mechanism of light collimation by leaky surface modes that propagate on a corrugated surface around the output of a photonic crystal waveguide. Analytical results obtained on the basis of the model are compared to those of rigorous numerical simulations. Maximum collimation is shown to occur at frequency values corresponding to excitation of surface modes whose wavenumber retains a *nonzero* real part.

PACS numbers: 42.70.Qs, 42.79.Ag, 78.68.+m

## I. INTRODUCTION

One of the problems hindering wider commercial application of photonic crystals (PCs) is the difficulty in coupling PC waveguides to conventional dielectric waveguides or optical fibers. A possible solution consists in tapering the waveguide so as to achieve better coupling with the fiber; this has been the subject of a number of publications, e.g., Ref. 1,2. Recently, Moreno *et al.*<sup>3</sup> and Kramper *et al.*<sup>4</sup> independently suggested that collimation of the light emitted by a waveguide (*beaming*) could also occur due to excitation of surface modes in the proximity of the waveguide exit. Based on the earlier discovery of a similar effect in metallic structures supporting surface plasmons<sup>5</sup>, the idea has been expanded in several articles following the original papers<sup>6,7,8,9,10,11</sup>.

Moreno *et al.* propose a simple qualitative theory to explain the novel effect<sup>3</sup>. The radiation reaching the waveguide outlet can couple to surface modes; if the surface around the outlet is *corrugated* (i.e., modulated with period different from that of the underlying crystal), its eigenstates become ‘leaky’, since energy is emitted as the radiation scatters at the perturbed surface cells. Under appropriate conditions, the scattered waves interfere constructively along the surface normal, thus producing a collimated beam. According to Ref. 3, this constructive interference takes place for surface modes of wavevector  $k_x = 0$  (shifted to the first Brillouin zone of the surface), so that the phase difference between two successive scatterers is equal to an integer multiple of  $2\pi$ .

The purpose of this work is to formulate a quantitative model of the beaming effect in PCs, taking explicitly into account the imaginary component of the leaky mode wavevector. The model predictions are tested against results of numerical simulations. We also show that, for practically realizable PCs, maximum beaming occurs for surface modes with  $\text{Re } k_x \neq 0$ .

## II. MODEL

The system to be considered is depicted in Fig. 1. Excited by a source at the waveguide input (left), a guided

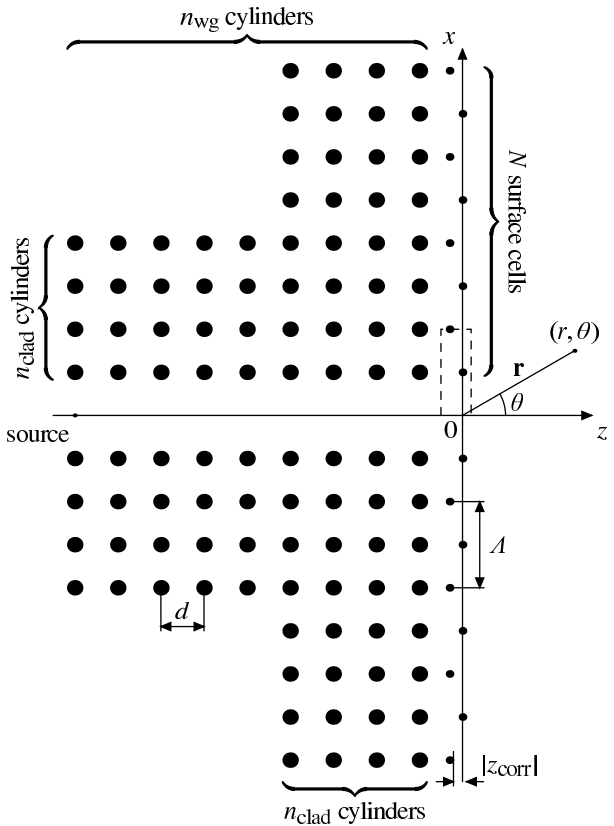


FIG. 1: A waveguide embedded in a PC with corrugated surface.

mode propagates towards the crystal surface (right). When reaching the output, the radiation is partially reflected, partially emitted directly into free space, and the remainder excites leaky modes propagating upwards and downwards along the corrugated surface. In this section we only focus on the latter fraction, assuming that the reflection coefficient varies slowly with frequency, and the fraction of energy emitted directly from the waveguide output is negligible. The validity of these assumptions is evaluated in Section IV.

The excited surface wave is characterized by its frequency  $\omega$  and its complex wavevector  $k_x \equiv k'_x + ik''_x$ , the

imaginary part of which is a measure of the scattering intensity. The surface cylinders are regarded as a periodic chain of point scatterers, which act as sources of cylindrical waves. Without losing generality, we restrict our attention to  $E$  polarization (with the electric field parallel to the cylinder axis). Our aim is to calculate the electric field  $E(\mathbf{r})$ , where  $r \equiv |\mathbf{r}|$  is assumed to be large compared to the system dimensions (the far-field limit).

We assume the crystal surface is corrugated with period  $\Lambda$  and either side of the waveguide comprises  $N$  elementary surface cells, each containing  $M$  scattering centres located at sites

$$\mathbf{r}_{nm}^\pm = x_{nm}^\pm \hat{\mathbf{x}} + z_{1m} \hat{\mathbf{z}} = \pm[(n-1)\Lambda + x_{1m}] \hat{\mathbf{x}} + z_{1m} \hat{\mathbf{z}}, \quad (1)$$

where  $n = 1, \dots, N$  represents the surface cell number,  $m = 1, \dots, M$  labels the scattering centre, and the signs  $+$  and  $-$  refer to cells above and below the  $z$  axis, respectively. For instance, the boxed surface cell in Fig. 1 contains two scatterers ( $M = 2$ ) at sites  $\frac{1}{2}\Lambda \hat{\mathbf{x}}$  and  $\Lambda \hat{\mathbf{x}} + z_{\text{corr}} \hat{\mathbf{z}}$ . The electric field stemming from the  $m$ th scatterer in the  $n$ th surface cell, at site  $\mathbf{r}_{nm}^\pm$ , is a cylindrical wave of amplitude proportional to the electric field incident on the scatterer:

$$E_{nm}^\pm(\mathbf{r}) = s \frac{e^{ik_0 |\mathbf{r} - \mathbf{r}_{nm}^\pm|}}{\sqrt{|\mathbf{r} - \mathbf{r}_{nm}^\pm|}} E_{nm}^{\pm, \text{inc}}, \quad (2)$$

where  $s$  is a proportionality constant describing the scattering intensity, and  $k_0 \equiv \omega/c$ . In the far-field limit,

$$\begin{aligned} |\mathbf{r} - \mathbf{r}_{nm}^\pm| &= \sqrt{(x_{nm}^\pm - r \sin \theta)^2 + (z_{1m} - r \cos \theta)^2} \\ &\approx r - (x_{nm}^\pm \sin \theta + z_{1m} \cos \theta) \\ &= r \mp [(n-1)\Lambda + x_{1m}] \sin \theta - z_{1m} \cos \theta \end{aligned} \quad (3)$$

and

$$\frac{1}{\sqrt{|\mathbf{r} - \mathbf{r}_{nm}^\pm|}} \approx \frac{1}{\sqrt{r}} \left( 1 + \frac{1}{2} \frac{x_{nm}^\pm \sin \theta + z_{1m} \cos \theta}{r} \right). \quad (4)$$

In the latter expansion we only need to keep the most slowly decaying term, i.e.,  $r^{-1/2}$ . Consequently, for large  $r$  values Eq. (2) becomes

$$\begin{aligned} E_{nm}^\pm(\mathbf{r}) &= s \frac{e^{ik_0 r}}{\sqrt{r}} e^{\mp ik_0 [(n-1)\Lambda + x_{1m}] \sin \theta} \\ &\times e^{-ik_0 z_{1m} \cos \theta} E_{nm}^{\pm, \text{inc}}. \end{aligned} \quad (5)$$

Through the application of the Bloch theorem,  $E_{nm}^{\pm, \text{inc}}$  can be written as

$$E_{nm}^{\pm, \text{inc}} = E_{1m}^{\pm, \text{inc}} e^{ik_x(n-1)\Lambda}; \quad (6)$$

for convenience,  $E_{1m}^{\pm, \text{inc}}$  can be given the following form:

$$E_{1m}^{\pm, \text{inc}} = u_m E_0 e^{ik_x x_{1m}}, \quad (7)$$

where  $E_0$  denotes the field incident at the first scatterer in the first unit cell ( $E_0 \equiv E_{11}^{\pm, \text{inc}} e^{-ik_x x_{11}}$ ), and the dimensionless quantity  $u_m$  ( $m = 1, \dots, M$ ) is a measure of the relative strength of the field incident on individual scatterers. As an example, consider the structure shown in Fig. 1. Scattering at subsurface layers can be neglected in the first approximation, in which, consequently, only the two surface cylinders per unit cell are taken into account. The electric field at both cylinders can reasonably be assumed to oscillate with equal amplitude, but in opposite phase; thus, we get  $u_1 = 1$  and  $u_2 = -1$ .

Including Eqs. (6) and (7) into Eq. (5), we get

$$\begin{aligned} E_{nm}^\pm(\mathbf{r}) &= s E_0 \frac{e^{ik_0 r}}{\sqrt{r}} u_m e^{i(k_x \mp k_0 \sin \theta) x_{1m}} e^{-ik_0 z_{1m} \cos \theta} \\ &\times e^{i(k_x \mp k_0 \sin \theta)(n-1)\Lambda}. \end{aligned} \quad (8)$$

For clarity reasons, let us introduce the *structure factor*  $F(\theta)$  and the *array factor*  $A(\theta)$ , defined as

$$F(\theta) \equiv \sum_{m=1}^M u_m e^{i(k_x - k_0 \sin \theta) x_{1m}} e^{-ik_0 z_{1m} \cos \theta}, \quad (9)$$

$$\begin{aligned} A(\theta) &\equiv \sum_{n=1}^N e^{i(k_x - k_0 \sin \theta)(n-1)\Lambda} \\ &= \frac{1 - e^{i(k_x - k_0 \sin \theta)N\Lambda}}{1 - e^{i(k_x - k_0 \sin \theta)\Lambda}}. \end{aligned} \quad (10)$$

Using these definitions, the total electric field at site  $\mathbf{r}$  is represented by the following sum of contributions of all the scatterers:

$$\begin{aligned} E(r, \theta) &= \sum_{n=1}^N \sum_{m=1}^M [E_{nm}^+(\mathbf{r}) + E_{nm}^-(\mathbf{r})] \\ &= s E_0 \frac{e^{ik_0 r}}{\sqrt{r}} [F(\theta) A(\theta) + F(-\theta) A(-\theta)] \\ &\equiv s E_0 \frac{e^{ik_0 r}}{\sqrt{r}} \mathcal{E}(\theta), \end{aligned} \quad (11)$$

$\mathcal{E}(\theta)$  denoting the term in square brackets.

From the Maxwell equations it can be shown that the radial component of the time-averaged Poynting vector,  $S_r(r, \theta)$ , is

$$S_r(r, \theta) = \frac{1}{2Z_0} |E(r, \theta)|^2 \quad \text{with} \quad Z_0 \equiv \sqrt{\frac{\mu_0}{\epsilon_0}}. \quad (12)$$

Consequently, the power radiated into an infinitesimal angle  $(\theta, \theta + d\theta)$  is

$$\Phi(\theta) d\theta = S_r(r, \theta) r d\theta = \frac{|s E_0|^2}{2Z_0} |\mathcal{E}(\theta)|^2 d\theta. \quad (13)$$

Integrated over the interval  $[-\frac{\pi}{2}, \frac{\pi}{2}]$ , this yields the total power radiated into free space:

$$P_{\text{rad}} = \frac{|s E_0|^2}{2Z_0} \int_{-\pi/2}^{\pi/2} |\mathcal{E}(\theta')|^2 d\theta'. \quad (14)$$

From the conservation of energy,

$$P_{\text{rad}} = P_0(1 - |\text{e}^{ik_x N \Lambda}|^2), \quad (15)$$

$P_0$  being the power exciting the surface modes. Using Eqs. (13)–(15), we normalize  $\Phi(\theta)$  to  $P_0$ , thus eliminating the coefficient  $|sE_0|^2$ . The final result reads

$$\frac{\Phi(\theta)}{P_0} = (1 - |\text{e}^{ik_x N \Lambda}|^2) \frac{|\mathcal{E}(\theta)|^2}{\int_{-\pi/2}^{\pi/2} |\mathcal{E}(\theta')|^2 d\theta'}. \quad (16)$$

Thus, the radiation intensity normalized to the accepted power is expressed solely in terms of the surface structure geometry and the leaky surface mode parameters.

### III. NUMERICAL DETERMINATION OF SURFACE MODES

To apply the above-discussed model to a specific photonic surface, e.g., for the determination of the frequency most favourable for beaming, it is necessary to calculate the dispersion relation of the modes supported by the surface. In this section we shall briefly outline the method we employed for this purpose.

In our approach, we consider a semi-infinite PC with possible surface reconstruction. The whole system is divided into three parts: the homogeneous region, the surface, and the underlying semi-infinite, but otherwise ideal, photonic crystal. The electromagnetic field in the homogeneous material is represented as the Rayleigh expansion, i.e., as a linear combination of discrete plane waves, whereas in the semi-infinite crystal the field is expanded into the eigenmodes of the corresponding infinite structure (a procedure suggested by Istrate *et al.*<sup>12</sup>). Since we are searching for surface-localized waves, in both regions we only consider waves that propagate or decay *away from the surface*. The complex band structure necessary to find the field representation in the PC is calculated by the differential method (see Ref. 13 for details).

The fields in the homogeneous region and in the PC are linked by the scattering matrix<sup>13</sup> of the surface layer, which provides the necessary boundary conditions. This leads to a homogeneous system of linear equations, which must have a non-trivial solution for the surface states to exist. The search for surface modes is thus reduced to a search for roots of the determinant of a matrix dependent on  $k'_x$ ,  $k''_x$  and  $\omega$ .

## IV. RESULTS

### A. Surface mode dispersion

In the following we will focus on crystals of the type shown in Fig. 1, considering a truncated square lattice of dielectric cylinders of permittivity  $\epsilon = 11.56$  embedded in vacuum, with bulk cylinder radius  $0.18d$ , surface

cylinder radius  $0.09d$ , surface corrugation period  $\Lambda = 2d$ , and three values of corrugation depth  $z_{\text{corr}}$ : 0,  $-0.1d$  and  $-0.3d$  (the minus sign indicating that the perturbed cylinders are shifted *towards* the crystal). For future reference, we denote these three crystals with letters *A*, *B*, and *C*, respectively. In Fig. 2 the dispersion curves of the surface modes supported by these crystals are plotted for small negative  $k'_x$ ; in this region, the mode group velocity is positive, which implies that  $k''_x \geq 0$ . The dispersion relations have been determined by the method described in the previous section.

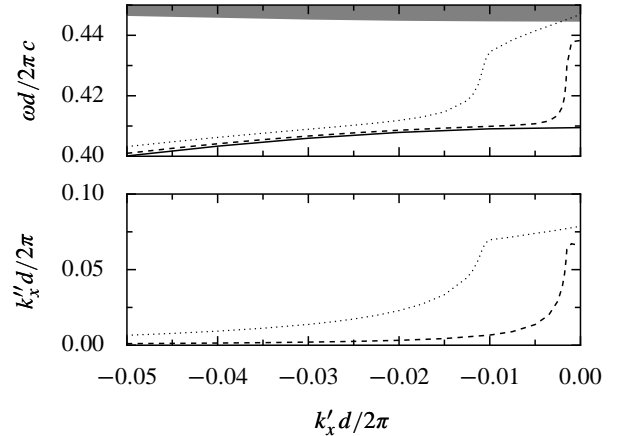


FIG. 2: Surface mode dispersion relation curves (top) and  $k''_x$  vs.  $k'_x$  plots for leaky surface modes (bottom) of crystals *A* (solid line), *B* (dashed line), and *C* (dotted line). The shaded region represents a bulk band.

The influence of corrugation on surface modes clearly increases as  $k'_x$  approaches zero, as evidenced by the large imaginary part of their wavevector, as well as by the significant change in mode frequency. This has been attributed to a stronger effect of scatterers on waves of low group velocity values<sup>10</sup>. Interestingly, for both corrugated surfaces analysed here (crystals *B* and *C*), the states corresponding to the immediate vicinity of point  $k'_x = 0$  are not truly localized, since the  $z$  component of their wavevector becomes purely real, even though the  $x$  component retains a large imaginary part. Figure 3 shows a juxtaposition of the electric field amplitude maps corresponding to a localized and a nonlocalized mode of crystal *B*.

### B. Light collimation: frequency dependence

We now proceed to the analysis of beaming itself. Figure 4 presents the electric field magnitude calculated by the multiple-scattering (MS) method (see Ref. 14 for details), with geometry parameters and frequency value favouring directional emission. In Fig. 5 the frequency dependence of the far-field radiation intensity  $\Phi_{\text{sim}}(\theta = 0)$  calculated by the MS method is compared to that obtained on the basis of our model, for crystals

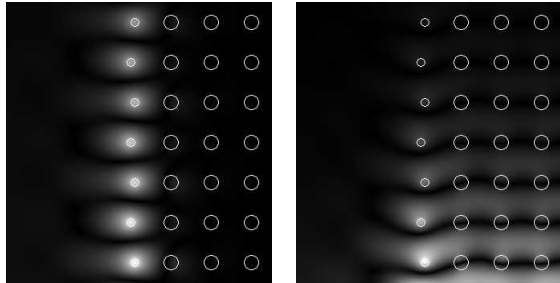


FIG. 3: Map of electric field magnitude for surface modes in crystal  $B$  at two reduced wavevector values:  $k_x \text{red} \equiv k_x d / 2\pi = -0.01 + 0.025i$  (left) and  $k_x \text{red} = 0 + 0.14i$  (right).

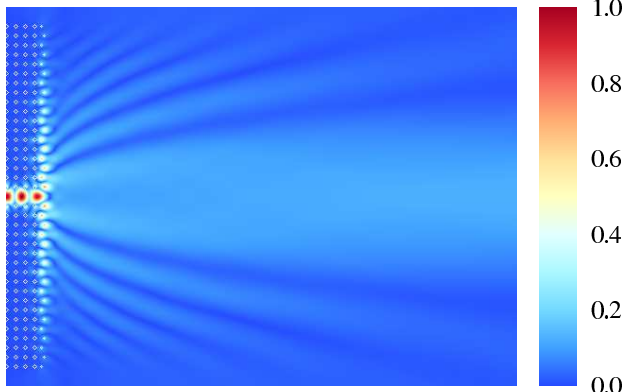


FIG. 4: (Color online) Electric field magnitude for crystal  $C$  with  $N = 9$  corrugated surface cells at reduced frequency  $\omega_{\text{red}} \equiv \omega c / 2\pi d = 0.410$ .

$B$  and  $C$  with  $N = 9$  and  $N = 15$  corrugations. In these MS simulations we consider the system depicted in Fig. 1, with the waveguide  $n_{\text{wg}} = 12$  cylinders long and cladding  $n_{\text{clad}} = 5$  cylinders wide; the waveguide mode is excited by a point source near the inlet. The results depicted in Fig. 5 clearly show that our model reproduces the basic feature of the effect in question, i.e., the existence of a distinct transmission maximum at a well-defined frequency value. Also the shape of the curves is rendered reasonably well within a broad frequency range. The better fit in the case of the longer surface ( $N = 15$ ) can be attributed to the fact that the amplitude of surface waves reflected at the crystal boundaries, neglected in our model, becomes smaller with increasing  $N$ . The effect of those waves is stronger in crystals with shallow surface corrugation (involving weakly leaky modes) and of small size (see Fig. 6).

The model does not reproduce correctly the relative heights of the  $\Phi_{\text{sim}}(\theta = 0)$  curve peaks for different crystals. This may stem from the simplifying assumption that the power  $P_0$  exciting the surface modes stays constant throughout the frequency range and does not depend on the corrugation depth. In reality, the waveguide-to-surface coupling may be sensitive to the precise structure of the region near the waveguide out-

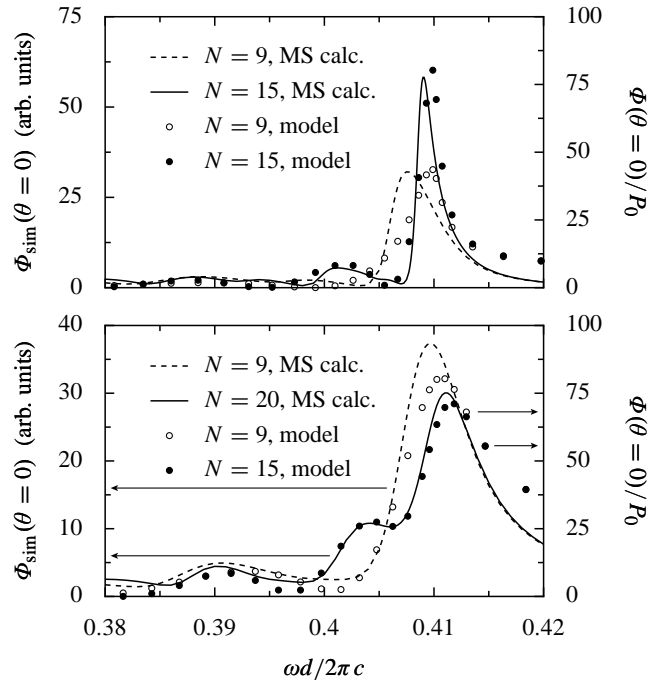


FIG. 5: Frequency dependence of the collimated beam intensity for crystal  $B$  (top) and  $C$  (bottom). The left and right  $y$  axes refer to the results of MS calculations (lines) and the model predictions (circles), respectively.

put. This dependence, however, is difficult to evaluate analytically.

### C. Light collimation: angular dependence

Figure 7 shows the angular dependence of  $\Phi(\theta)/P_0$  as predicted by our model and, for comparison, the data obtained by the MS method for crystal  $C$  with  $N = 9$  corrugations at reduced frequency  $\omega_{\text{red}} \equiv \omega c / 2\pi d = 0.400$ . The overall shape of the curve is well reproduced: in agreement with the simulations, our theory predicts an intensity minimum at  $\theta = 0$ , two symmetric principal maxima at low angles, and a number of minor sidelobes; however, the positions of individual peaks are shifted several degrees away from the  $x$  axis. The fit quality can be significantly improved by taking into account the light radiated directly from the waveguide outlet, which can be approximately regarded as stemming from a point source placed at the origin of the coordinate system shown in Fig. 1. The grey curve in Fig. 7 shows the theoretical  $\Phi(\theta)/P_0$  dependence with this additional point source included in the sum in Eq. (11), its phase and magnitude chosen so as to obtain the best fit. Clearly, even this crude representation of the field stemming from the waveguide outlet results in a visible improvement of match quality; in particular, the sidelobe position discrepancy is eliminated.



FIG. 6: Electric field magnitude in the surface region of crystal  $B$  with  $N = 9$  corrugations at reduced frequency  $\omega_{\text{red}} = 0.405$ . An interference pattern resulting from surface wave reflections at the crystal boundaries is clearly visible.

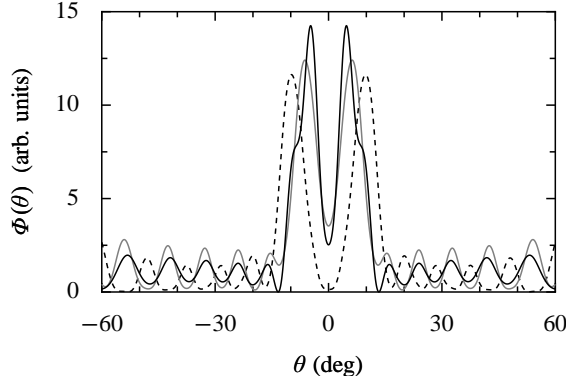


FIG. 7: Angular dependence of the far-field radiation intensity for crystal  $C$  with  $N = 9$  corrugations at reduced frequency  $\omega_{\text{red}} = 0.400$ . Solid black line: MS simulations; dashed line: model predictions without including the field emitted directly from the waveguide output; grey line: model predictions with this field taken into account (see text). The theoretical curves have been scaled by adjusting the  $P_0$  factor so as to obtain the best fit.

## V. DISCUSSION

As indicated in Fig. 5, maximum beam collimation occurs at reduced frequency of around 0.41, which, according to Fig. 2, corresponds to surface modes with  $k'_x \text{red} \equiv k'_x d / 2\pi \approx -0.01$  (crystal  $B$ ) and  $k'_x \text{red} \approx -0.025$  (crystal  $C$ ) *rather than* to modes from the centre of the Brillouin zone ( $k'_x = 0$ ). Incidentally, the  $k'_x = 0$  mode, being delocalized, could not be responsible for beaming. However, the nonzero real part of the wavevector of the surface mode for which maximum beaming is observed is easily explained on the basis of the model discussed in Section II. It is a consequence of the competition between the tendency to reduce  $|k'_x|$  in order to obtain better phase-matching of the waves diffracted at the individual scatterers, and, on the other hand, the negative effect of too large a  $k''_x$  on the effective length of the ‘grating’. Since a decrease in  $|k'_x|$  is always accompanied by an increase in  $k''_x$ , the most intensive beaming occurs for moderate (‘balanced’) values of both parameters.

The model also sheds new light on the fact that, for negatively corrugated crystals, the frequency value corresponding to maximum beaming lies remarkably close to

that of the unperturbed surface mode from the Brillouin zone centre. This proves to be a resultant of two opposing effects. It has been pointed out<sup>10</sup> that bringing surface cylinders closer to the bulk crystal causes a blueshift of the surface mode dispersion relation, due to a decrease of the fraction of electromagnetic energy contained within the dielectric. However, since beaming occurs at nonzero  $k'_x$  values, the shift starts from an initial frequency value lower than that of the Brillouin-zone-centre mode. In sum, the resultant optimum beaming frequency is close to the original frequency of the  $k'_x = 0$  mode.

The model proposed in this paper can be easily extended to take into account scattering by subsurface layers, as well as the surface wave reflections at the crystal boundaries. Both effects do not lead, however, to qualitatively different results. A detailed investigation of the interactions between the waveguide output and the surface cylinders in its immediate vicinity could help improve the accuracy of the model, as these interactions determine the amount of power transferred to surface modes and that emitted directly into free space. An analytical formulation of these effects, however, seems hardly feasible.

## VI. CONCLUSIONS

We have presented a quantitative analysis of a model explaining the effect of surface corrugation on the collimation of radiation leaving the outlet of a photonic crystal waveguide. Besides clarifying the conditions necessary for optimum beaming, the model also explains the relative insensitivity of the frequency value at which maximum collimation takes place to the degree of surface modulation. We believe our results will contribute to a deeper understanding of the physical grounds of the beaming effect.

### Acknowledgments

I thank Prof. Henryk Puszkarz and Dr. Maciej Krawczyk for numerous useful discussions and encouragement during my work on this project.

\* Electronic address: achu@hoch.amu.edu.pl

<sup>1</sup> A. Mekis and J. D. Joannopoulos, *J. Lightwave Technol.*

<sup>1</sup> **19**, 861 (2001).

<sup>2</sup> A. Hakansson, P. Sanchis, J. Sánchez-Dehesa, and J. Martí, *J. Lightwave Technol.* **23**, 3881 (2005).

<sup>3</sup> E. Moreno, F. J. García-Vidal, and L. Martín-Moreno, *Phys. Rev. B* **69**, 121402 (2004).

<sup>4</sup> P. Kramper, M. Agio, C. M. Soukoulis, A. Birner, F. Müller, R. B. Wehrspohn, U. Gösele, and V. Sandoghdar, *Phys. Rev. Lett.* **92**, 113903 (2004).

<sup>5</sup> H. J. Lezec, A. Degiron, E. Devaux, R. A. Linke, L. Martín-Moreno, F. J. García-Vidal, and T. W. Ebbesen, *Science* **297**, 820 (2002).

<sup>6</sup> E. Moreno, L. Martín-Moreno, and F. J. García-Vidal, *Photonics and Nanostructures* **2**, 97 (2004).

<sup>7</sup> W. R. Frei, D. A. Tortorelli, and H. T. Johnson, *Appl. Phys. Lett.* **86**, 1114 (2005).

<sup>8</sup> S. K. Morrison and Y. S. Kivshar, *Appl. Phys. Lett.* **86**, 1110 (2005).

<sup>9</sup> S. K. Morrison and Y. S. Kivshar, *Appl. Phys. B* **81**, 343 (2005).

<sup>10</sup> S. K. Morrison and Y. S. Kivshar, *Proc. SPIE* **5733**, 104 (2005).

<sup>11</sup> I. Bulu, H. Caglayan, and E. Ozbay, *Opt. Lett.* **30**, 3078 (2005).

<sup>12</sup> E. Istrate, A. A. Green, and E. H. Sargent, *Phys. Rev. B* **71**, 195122 (2005).

<sup>13</sup> E. Popov and B. Bozhkov, *Appl. Opt.* **39**, 4926 (2000).

<sup>14</sup> D. Felbacq, G. Tayeb, and D. Maystre, *J. Opt. Soc. Am. A* **11**, 2526 (1994).